

LCLS UNDULATOR DESIGN DEVELOPMENT

Isaac Vasserman, Roger Dejus, Patric Den Hartog, Elizabeth Moog, Shigemi Sasaki, Emil Trakhtenberg, Marion White, ANL/APS, Argonne, Illinois 60439, USA

Abstract

The undulator segments of the 130.4-m-long undulator line for the Linac Coherent Light Source project (LCLS) [1] must have a deflection parameter K_{eff} that matches the nominal value for that segment to within $\Delta K_{eff}/K_{eff} < 1.5 \times 10^{-4}$. Mechanical shims were used to set the undulator gap to control K in the prototype, but this is too tedious a procedure to be used for all 33 undulator segments. Although the prototype undulator [2-4] met all of the LCLS specifications, development continued in order to simplify the system. Various other alternatives for adjusting the field were considered. A canted-pole geometry was chosen, allowing the K value to be changed by lateral translation of the entire undulator segment. This scheme also facilitates tapering the undulator line to accommodate electron beam energy loss. The prototype undulator was subsequently modified to test the canted-pole concept. Magnetic measurements demonstrated that the undulator with canted poles meets all LCLS specifications, and is more cost effective to implement.

INTRODUCTION

The LCLS prototype undulator cross section is shown in Fig. 1. Wedged spacers are located between the titanium core and the aluminum bases. Translation of a canted undulator segment in the transverse horizontal direction (X) allows the desired K_{eff} to be achieved with the required accuracy during initial tuning.

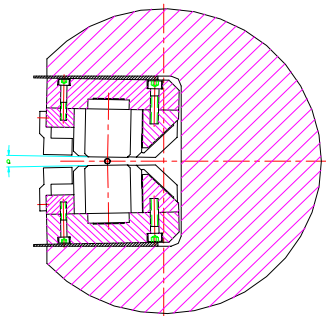


Figure 1: LCLS prototype cross section for the modified design with canted pole-gap.

Remote control of the device's X position can serve to keep the field stable despite temperature changes. It can also be used to tune the phase between devices when particle energy loss has disrupted the phasing. The range of X motion could be as large as ± 5 mm to compensate for the beam energy loss at saturation. It is important to keep

the performance (phase errors, trajectory straightness, etc.) of the undulator segments within the required tolerances [1] in this wide transverse position range. To confirm that this can be done, the LCLS prototype undulator was modified to introduce a 3-mrad cant. Measurements of the rms phase errors, K_{eff} and the X -dependence of the field integrals are described below. Alignment of the magnetic elements is critical for this project. The option of using magnetic needles to locate the magnetic center of the undulator segment is discussed. Additional design changes that were implemented recently are described elsewhere [5].

MAGNETIC MEASUREMENT OF THE PROTOTYPE UNDULATOR

Phase Errors

The LCLS undulator will use the first harmonic of the radiation so its output is not very sensitive to phase errors between the particle beam and radiation [6-8]. The allowable upper limit of rms phase errors is 6.5° . The X dependence of the rms phase error was measured in the range of ± 3 mm and was found to be negligible.

Effective Field

Figure 2 shows the X dependence of the effective field (B_{eff}) and the effective deflection parameter (K_{eff}). This dependence is linear in X , and close to the 1.9 G/ μm previously measured for the gap dependence. The difference can be attributed to the initial wedging in the pole gap created by pole sorting to allow for easy gap measurement [3].

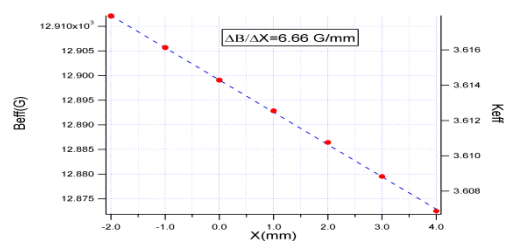


Figure 2: B_{eff} and K_{eff} dependence on X . $\Delta X = 0.3$ mm corresponds to the alignment accuracy needed for the tolerance $\Delta B_{eff}/B_{eff} = 1.5 \times 10^{-4} \sim 2$ Gauss.

The 3-mrad cant is small so that the alignment accuracy required in the X direction, 0.3 mm, is not difficult to achieve. With this cant angle, the change in field strength

due to a temperature change of 1°C can be compensated by a lateral shift of the undulator segment by 1.2 mm, which can be done remotely.

Horizontal and Vertical Trajectories

The horizontal trajectories for different X positions in the range of ± 3 mm are shown in Fig. 3.

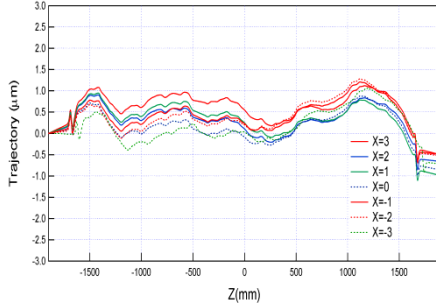


Figure 3: Horizontal trajectories at different X positions for a beam energy of 14.1 GeV.

The trajectories are well behaved and well within the tolerance requirement of 2 μm maximum walk-off from a straight line for a particle energy of $E=14.1$ GeV. The change in the vertical field integrals can be calculated from Maxwell's equation $\partial B_y / \partial x = -\partial B_x / \partial y$, using the horizontal trajectory measurements. Final tuning of the undulator segments may require tuning of the vertical trajectories as well.

Magnetic Field Fine Tuning

The method for adjusting K_{eff} is: a) Select among spacers with thickness step ~ 15 μm to set the effective field within ± 30 G (1 μm in gap corresponds to ~ 2 Gauss in field); b) Set the horizontal position of the spacers to adjust the effective field to $\sim \pm 6$ Gauss (for a 3-mrad cant, 6 G corresponds to a 1-mm shift in horizontal position); c) Set the horizontal position of the undulator segment as a whole so that the effective field is in the range of ± 2 G ($\Delta B_{\text{eff}} / B_{\text{eff}} \sim \pm 1.5 \times 10^{-4}$). The last step saves shimming time and provides better accuracy.

PHASE TUNING

The phase slippage along the undulator can be calculated using [9]:

$$\varphi(z) = \frac{k}{2\gamma^2} \left[z + \int_0^z I_{1x}^2(z') dz' + \int_0^z I_{1y}^2(z') dz' \right], \text{ where}$$

k is the fundamental harmonic wave-vector of the radiation, γ is the relativistic factor, and I_{1x} and I_{1y} are the normalized particle angles in the vertical and horizontal directions, respectively. In free space, with zero field and zero angle we have:

$$\varphi(z) = \frac{k}{2\gamma^2} z, \quad L_{\text{free}} = n\lambda_u (1 + K_{\text{eff}}^2 / 2), \quad \text{where}$$

L_{free} is the required distance in free space for n periods of phase slippage. An initial magnetic tuning will be

required for each undulator segment to match its phasing to the standard mechanical break length. Full-width magnet shims (phase shims) will be applied to correct the field, if needed. Such shims were successfully used in the APS FEL project. The result of the phase shim test is shown in Fig. 4. The physical break length will be chosen to match what is typical for an undulator with six phase shims. This will allow adjustment in either direction. Other ways of tuning break length, such as K_{eff} tuning and trajectory shims, will be used if necessary.

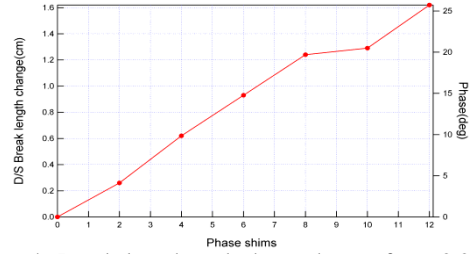


Figure 4: Break length and phase change from 0.2-mm-thick phase shims applied at one end of the undulator. The first two shims were applied to magnet #7, one each on the top and bottom jaws, the next two to magnet #6, etc.

Particle energy loss results in a change of phase in and between the undulator segments that must be corrected. The estimated energy loss in the first 100 m of undulator is 0.26%; 0.4% is estimated for the last 30 m with saturation [1]. The resulting phase slippage in the undulator segment can be corrected by remotely changing the K_{eff} of the undulator segment. The phase change in the drift space must also be corrected. The previous prototype undulator design had active end-gap corrections to correct the phasing, but modifying K_{eff} instead is simpler. Tests were conducted to demonstrate the feasibility.

Polar plots based on the complex radiation amplitude are powerful tools in understanding phasing issues. The complex radiation amplitude A is defined as [9]:

$$A(z) = \int_0^z I_{1y}(z') e^{-i\varphi(z')} dz'.$$

The magnitude of A is plotted as the radius, and the complex phase angle of A is plotted as the angle. These values, calculated for a sequence of points along the undulator, are plotted. A properly phased undulator will be represented as a straight line, radially outward from the center of the graph. Phasing errors appear as curved lines or kinks. The absolute value of the complex radiation amplitude at the undulator segment end $A(L)$ is represented in the polar plot as the distance between the initial and final points of the vector. The radiation intensity is proportional to $|A|^2$.

Consider the case with a long line of ideal undulators and ideal particle beam energy, followed by two undulators separated by a long break section with three periods of phase slippage in the drift space. Also, assume that the particle beam energy is 0.4% too low through those two undulators, due to a beam energy loss. Figure 5 is a polar plot through those two undulators and the drift

space between them. The line curvature is so extreme that the radiation intensity from the two undulators is sharply reduced. The performance of the undulator is seen to be very sensitive to the particle energy.

The curvature in Fig. 5 can be understood because spontaneous radiation from the undulators and the reduced particle beam energy would not be at the nominal wavelength. Figure 6 shows what happens when the magnetic field strength of the two undulators is adjusted so the spontaneous radiation is at the nominal wavelength, despite the reduced beam energy. The traces through the two undulators are straight, as they should be, but now there is a kink between the two undulators, showing that the drift space is not the right length for the reduced beam energy. This type of plot can clearly show and help diagnose the origin of an effect that only impacts the final radiation amplitude by 2% of the ideal value.

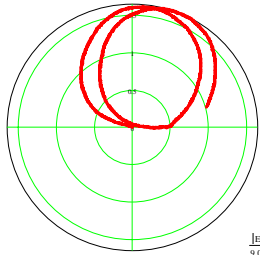


Figure 5: After passing through a line of undulator segments where the undulators are perfect and the beam energy is ideal, the beam loses 0.4% of its energy prior to passage through two undulators that are separated by a drift space with three periods of phase slippage. The magnitude and complex phase angle of A are plotted in polar coordinates at points along the two undulators. The radiation amplitude from those two undulators, represented by the length of a vector from the beginning to the end of the trace, is very small.

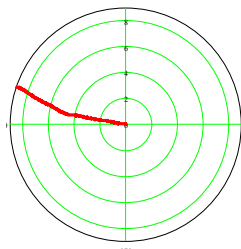


Figure 6: Same type of plot as in Fig. 5. The K_{eff} of the two undulators has been adjusted so that the spontaneous radiation is at the nominal wavelength, despite the beam energy loss. The lines through the undulators are straight, and the kink between them indicates a phasing error in the drift space. The radiation amplitude from these undulators is now 98.2% of ideal.

An additional improvement can be obtained if, instead of adjusting K_{eff} to match the spontaneous radiation to the nominal wavelength, K_{eff} is adjusted to maximize the overall $|A|$. The polar plot resulting from such a change is shown in Fig. 7. As can be seen by the curvature in the traces through the undulators, there is a small phase

slippage in the undulator segments, but the net effect is that the radiation amplitude is 99.1% of ideal.

It may at some time be desirable to remove an undulator segment from the undulator line. An issue that must be considered before doing so, however, is what becomes of the phasing between the undulator segments immediately upstream and downstream of the removed one. If the new undulator-long drift space is the same length as an integer number of free-space slippage lengths, then the phasing between the adjacent undulator segments will be good. (Some steering correction may be needed, however, to compensate for the environmental magnetic field.) If, as is more likely, the drift length isn't right, resulting in a phase error, then an adjustment of the K_{eff} of the undulators may be able to compensate.

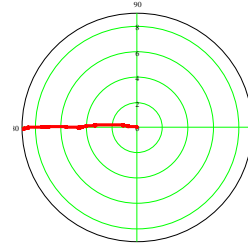


Figure 7: Same as Fig. 6, but with K_{eff} of the two undulators adjusted to maximize the overall $|A|$. The K_{eff} through the undulators is not perfect, as can be seen by the slight curvature, but the overall $|A|$ is 99.1% of ideal.

An example of such an adjustment is shown in Fig. 8. When $K_{eff} = 3.62$, the drift-space length is nearly an integer number of slippage lengths so the required K_{eff} adjustment is small. Another example is shown in Fig. 9 for nominal $K_{eff} = 3.44$. (The electron beam energy is also changed, to keep the wavelength of the radiation at 1.5 Å.) At this new nominal K_{eff} , the drift space length is nearly perfectly wrong, so even tuning K_{eff} is not enough. The phasing correction would be easier in this case if two undulators were removed.

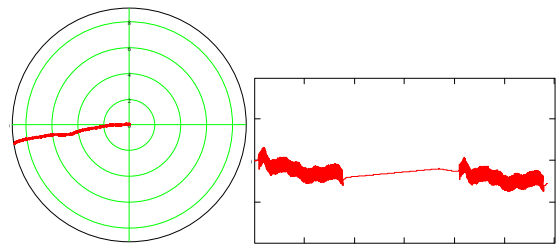


Figure 8: Polar plot (left) and trajectory (right) with one device removed. K_{eff} was changed by 0.03% (0.6-mm shift in X) to compensate for the phase distortion in the drift space. Nominal $K_{eff} = 3.62$. $|A|$ is 99.3% of ideal for two undulators.

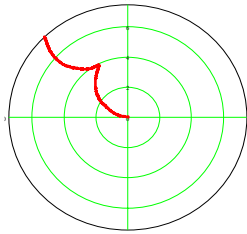


Figure 9: Same as Fig. 8 but with nominal $K_{eff} = 3.44$. The drift space length is 17.54 slippage lengths, making the second undulator almost exactly out of phase. $|A|$ was optimized by a 0.16% change in K_{eff} (3.2-mm shift in X), but still only 81.6% of ideal was reached.

MAGNETIC NEEDLES

With a canted gap undulator, accurate alignment in both the horizontal and vertical directions is critical, and a method to accomplish this has been studied. The magnetic center of the undulator can be determined using a Hall probe. The position of the Hall probe's sensitive area is difficult to determine, therefore the probe will be used to relate the undulator magnet centerline to positions of magnetic needles attached to the undulator.

A Sentron Hall probe was used to scan past a magnetic needle and the results are shown in Figs. 10 and 11.

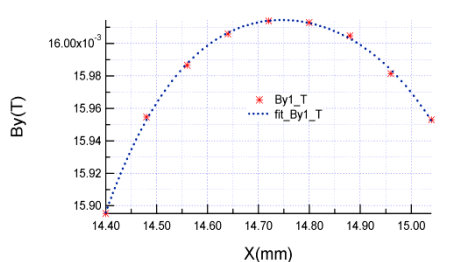


Figure 10: Horizontal scan past the tip of a vertical-pointing magnetic needle.

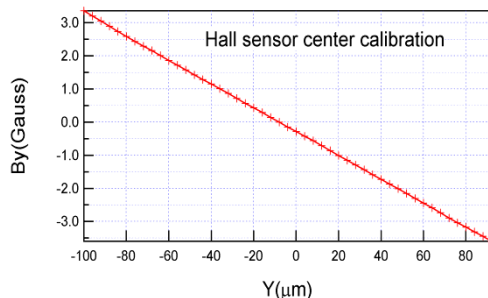


Figure 11: Vertical scan past the tip of a horizontal-pointing magnetic needle. The magnetic center of the undulator is at $y = 0$. $By = 0$ is the center of the needle. The distance between them can be determined from the plot to within $5 \mu\text{m}$.

The vertical field distribution along the X -axis is shown in Figure 10. The spacing between data points was determined by the $50\text{-}\mu\text{m}$ encoder resolution. An encoder

with finer resolution will be used in the final system. Alignment in the Y direction is shown in Fig. 11. The needle points horizontally in this case, and the Hall probe scan direction is vertical. The magnetic center of the undulator is at $y = 0$. $By = 0$ is the center of the needle. The distance between them can be determined from the plot to within $5 \mu\text{m}$.

SUMMARY

Wedged spacers were inserted between the aluminum base plates and the titanium strongback of the existing LCLS prototype undulator, to give a 3-mrad cant to the pole gap. (A 4.5-mrad cant has since been determined to be preferred for the final LCLS undulator.) The measured variation of the magnetic field with horizontal position was as expected, making it possible to move the undulator laterally to adjust the on-axis field strength. The rms phase error did not change significantly with X , so the undulator can be used at different lateral positions. Coarse adjustment of the field strength can be done by the choice of spacer thickness, and by sliding the chosen spacer horizontally. The fine adjustment will be accomplished by lateral translation of the undulator. Horizontal translation of the undulator can also be used to correct the temperature dependence of the field strength. Magnetic needles were found to be effective alignment tools.

ACKNOWLEDGMENTS

The authors would like to thank Dr. J. Pflueger for his suggestion to cant the undulators. This work is supported by the U.S. Department of Energy, Office of Basic Energy Sciences, under Contract No. W-31-109-ENG-38.

REFERENCES

- [1] Coherent Light Source Project, SLAC-R-593, April 2002, <http://www-ssrl.slac.stanford.edu/lcls/cdr/>.
- [2] E.R. Moog et al, "Design and Manufacture of a Prototype Undulator for the LCLS Project," Proc. of PAC 2001, Chicago, June, 2001.
- [3] I.B. Vasserma et al., "Magnetic measurements and tuning of the LCLS prototype undulator," Nucl. Instrum. Methods A, 507 (2003) 191-195.
- [4] LCLS Prototype Undulator Report, R.J. Dejus, editor, ANL/APS/TB-48 (2004).
- [5] E. Trakhtenberg et al., "Undulators for the LCLS Project - from the prototype to full-scale manufacturing," XV Int'l. Synchrotron Radiation Conf., July 19-23, Novosibirsk, Russia (2004).
- [6] B.M. Kincaid, J. Opt. Soc. Am. B, 2 (1985) 1294.
- [7] B. Diviacco, R.P. Walker, Nucl. Instrum. Methods A, 368 (1996) 522.
- [8] L.H. Yu et al., Phys. Rev. A, 45 (1992) 1163.
- [9] E. Gluskin et al., Nucl. Instrum. Methods A, 475 (2001) 323.